ELSEVIER

Journal of Crystal Growth 223 (2001) 383–388

JOURNAL OF CRYSTAL GROWTH

www.elsevier.nl/locate/jcrysgro

Crystal growth of Ce-doped and undoped $LiCaAlF_6$ by the Czochralski technique under CF_4 atmosphere

Kiyoshi Shimamura[a,*], Sonia L. Baldochi[a], Izilda M. Ranieri[a], Hiroki Sato[a], Tomoyo Fujita[a], Vera L. Mazzocchi[c], Carlos B.R. Parente[c], Carlos O. Paiva-Santos[b], Celso V. Santilli[b], Nobuhiko Sarukura[d], Tsuguo Fukuda[a]

[a] *Institute for Materials Research, Tohoku University, Sendai 980-8577, Japan*
[b] *Instituto de Quimica, UNESP, Brazil*
[c] *Instituto de Pesquisas Energéticas e Nucleares-IPEN/CNEN-SP, Brazil*
[d] *Institute for Molecular Science, Okazaki 444-8585, Japan*

Received 25 November 2000; accepted 4 December 2000
Communicated by M. Schieber

Abstract

Ce-doped and undoped $LiCaAlF_6$ (LiCAF) single crystals 50 mm in diameter were grown by the Czochralski technique. The formation of inclusions and cracks accompanying the crystal growth was investigated. The dependence of lattice parameters on the temperature was measured for LiCAF and $LiSrAlF_6$ single crystals. Linear thermal expansion coefficients for both these crystals were evaluated. Higher transmission properties for LiCAF single crystals were achieved in the UV and VUV wavelength regions.

Keywords: A1. Growth from melt; A2. Czochralski method; B1. Halides

1. Introduction

Ce-doped Colquiriite-type fluoride single crystals such as $LiCaAlF_6$ (Ce : LiCAF) and $LiSrAlF_6$ (Ce : LiSAF) have been reported as leading candidates for tunable all-solid-state lasers in the UV wavelength region [1,2]. Recently, their high potential as optical window materials in the ultraviolet (UV) and vacuum-ultra-violet (VUV) wavelength regions was also identified [3] based on their short absorption edges.

We have previously reported the growth of 18 mm diameter Ce : LiCAF and Ce : LiSAF single crystals without the use of HF gases or the hydrofluorination of raw materials [3,4]. High laser performance with an output energy of 60 mJ was achieved using Ce : LiCAF crystals grown in this way [5]. The growth of 1 in Ce : LiCAF single crystals under CF_4 has also been reported. In order to avoid the formation of inclusions and cracks and enable growing high-quality crystals with higher reproducibility, several crystal growth conditions have been optimized [6–9].

*Corresponding author. Tel.: +81-22-215-2103; fax: +81-22-215-2104.
E-mail address: shimak@lexus.imr.tohoku.ac.jp (K. Shimamura).

0022-0248/01/$ - see front matter
PII: S0022-0248(01)00593-0

In the present work, we describe the growth of 2″ Ce : LiCAF single crystals by the Czochralski (CZ) technique under modified growth conditions based on the investigations of Shimamura et al. [3]. Problems accompanying crystal growth, such as inclusions and cracks, were investigated. The transmission property in the UV and VUV wavelength regions was improved as well as the crystal quality.

2. Experiment

Crystal growth was performed in a CZ system with a resistive heater made of high-purity graphite. Detailed processes for the preparation of raw materials and crystal growth are described in Ref. [3]. For the growth of 2″ crystals, a Pt crucible 100 mm in diameter was used. Growth orientation was controlled using *a*-axis oriented seed crystals. The pulling rate was 0.8 mm/h and the rotation rate was 10 rpm.

The dependence of lattice parameters on the temperature was measured by the high temperature X-ray powder diffraction method using a RIGAKU RINT 2000 apparatus under vacuum atmosphere. Specimens for XRD analysis were prepared by milling grown single crystals in a mortar. The distribution of bi-refringence among wafers was measured by the rotating analyzer method using an ELP-UV apparatus, under 266 nm illumination. Specimens for this experiment were prepared by cutting grown crystals normal to the $\langle 1\,0\,0\rangle$ orientation to a thickness 10 mm. Transmission in the VUV wavelength region at room temperature was analyzed by VUV 5530 spectrophotometry under vacuum. Wafers with (1 0 0) orientation for this analysis were made by cutting grown crystals and polishing.

3. Results and discussion

Fig. 1 shows typical as-grown 25 mm diameter Ce : LiCAF and Ce : LiSAF crystals. Although Ce : LiCAF single crystals can be grown reproducibly without inclusions and cracks, Ce : LiSAF crystals have shown a tendency to crack and to include inclusions under the same growth conditions as Ce : LiCAF crystals, as shown in Fig. 1(b).

Fig. 2 shows the dependence of the lattice parameters *a* and *c* on the temperature. In the case of LiCAF crystals, at a temperature below 600°C, only the LiCAF phase existed, while above 700°C, the compound was completely decomposed to Li_3AlF_6, CaF_2 and Al_2O_3. It was considered that Al_2O_3 was synthesized by the presence of a small amount of water or oxygen in the system. Therefore, thermal expansion was evaluated only up to 600°C. LiSAF crystals also showed the same phenomena as LiCAF. The calculated linear thermal expansion coefficients α_{11} and α_{33} are listed in Table 1. There is a notable difference between the linear thermal expansion coefficient along the *a*-axis and along the *c*-axis of LiCAF crystals. The latter is $\alpha_{33} = 2.5 \times 10^{-6}\,^{\circ}C^{-1}$, which is only about 10% of the former, $\alpha_{11} = 22.9 \times 10^{-6}\,^{\circ}C^{-1}$. Further, the thermal expansion of LiSAF was highly anisotropic, due to the thermal expansion along the *c*-axis being negative,

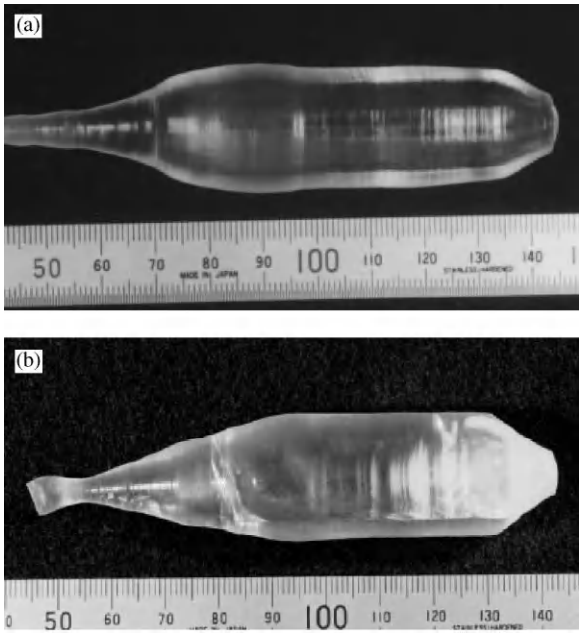

Fig. 1. As-grown 25-mm diameter Ce-doped (a) $LiCaAlF_6$ and (b) $LiSrAlF_6$ crystals pulled along the *a*-axis.

i.e. the lattice parameter c decreases with increasing temperature. These results suggest that large diameter LiSAF crystals are difficult to grow from the melt because of thermal stress inside the grown crystals. No distinct difference in the linear thermal expansion coefficients was observed between undoped crystals and Ce-doped ones. Based on these considerations, 2″ LiCAF single crystals have been investigated.

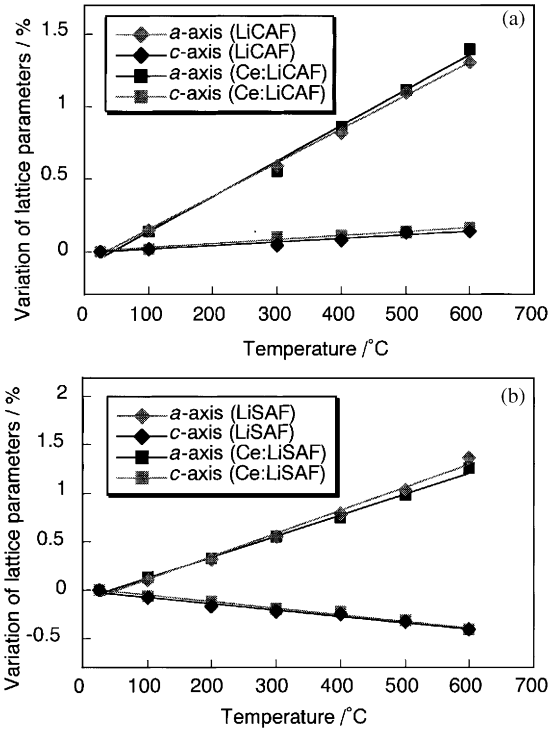

Fig. 2. Temperature dependence of the lattice parameters a and c for (a) $LiCaAlF_6$ and (b) $LiSrAlF_6$ single crystals.

When 2″ diameter crystals were grown, the following two problems appeared: the formation of inclusions, and cracks accompanied by the formation of an impurity phase at the bottom of the crystal.

Fig. 3 shows an as-grown Ce : LiCAF crystal which contains inclusions. Many inclusions are distributed throughout the crystal. It should be noticed that the formation of these inclusions was related to a change in the crystal diameter, for example at the shoulder of the crystal. Once they appeared at the shoulder, they did not disappear during crystal growth. In order to avoid these inclusions, the diameter at the shoulder should be controlled precisely and extended smoothly, without a rapid diameter change. Fig. 4 shows a SEM image of typical inclusions observed inside the as-grown Ce : LiCAF crystal. Foreign substances several microns in size could be seen precipitated inside the boules. The chemical composition of the

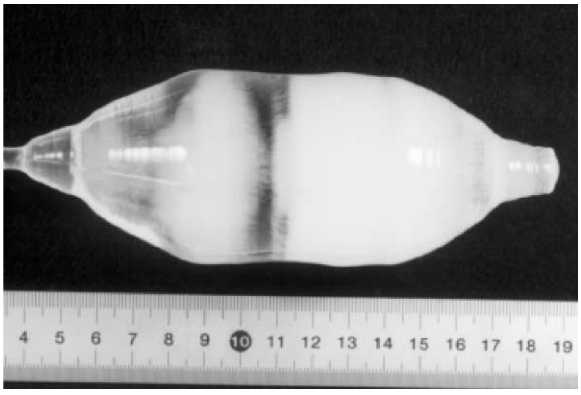

Fig. 3. As-grown 2″ Ce-doped $LiCaAlF_6$ crystal with inclusions.

Table 1
Linear thermal expansion of undoped and Ce-doped $LiCaAlF_6$ and $LiSrAlF_6$ single crystals

	Linear thermal expansion coefficients ($\times 10^{-6}$ °C^{-1})	
	α_{11} (along the a-axis)	α_{33} (along the c-axis)
$LiCaAlF_6$	22.9	2.5
$LiSrAlF_6$	23.5	−6.6
Ce : $LiCaAlF_6$	24.3	2.7
Ce : $LiSrAlF_6$	21.6	−6.7

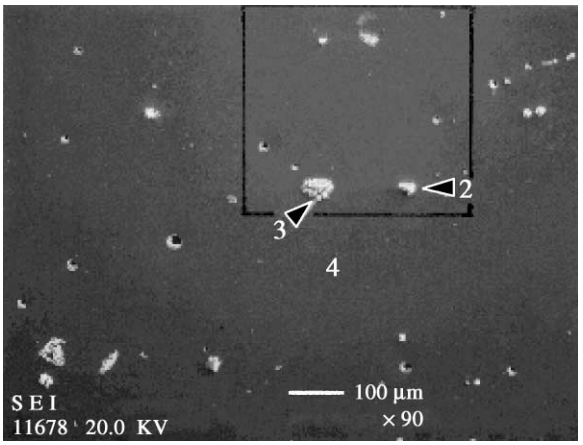

Fig. 4. SEM image of typical inclusions observed in the Ce : $LiCaAlF_6$ crystals, using secondary electron imaging.

Table 2
Chemical composition of inclusion compared with crystal matrix

	Matrix (wt%)	Inclusion (wt%)
Li	3.66	—
Ca	19.4	24.9
Al	14.4	0.10
F	62.5	35.8
Ce	0.002	40.5

inclusions was measured by EPMA technique. Table 2 shows the result of chemical composition analysis. From the results of quantitative analysis, it was found that these inclusions were composed of an excess of the Ce and Ca components. This also shows that the inclusions observed in the undoped LiCAF crystals are composed of an excess of the Ca component.

Fig. 5 shows an as-grown crystal with one large crack along the growth axis and a white substance at the bottom of the crystal. This large, flat crack appeared during cooling after growth when the white material was present. This white substance usually formed when the solidification fraction exceeded 70%. The XRD analysis showed that the white substance was composed of LiCAF and CaF_2 phases. This is because the melt composition shifted in the CaF_2-enriched direction during growth, since the vaporization pressure of LiF and AlF_3 is very high [10]. CeF_3 and NaF might have accumulated in the residual melt due to the small k_{eff} [3]. In order to avoid the formation of this white substance, crystal growth was terminated at the solidification fraction of 60%. For further improvement, optimization of melt composition should be carried out.

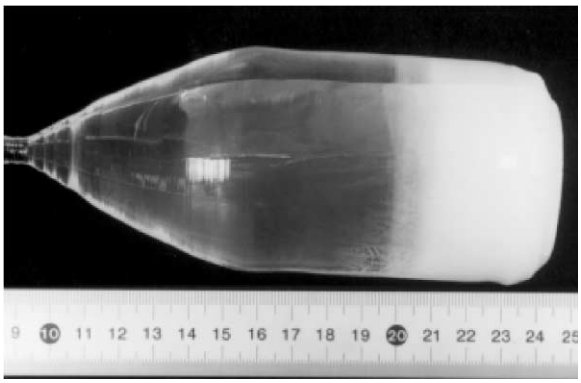

Fig. 5. As-grown 2″ Ce-doped $LiCaAlF_6$ single crystal with white substance at the bottom of the crystal and a large crack parallel to the growth axis.

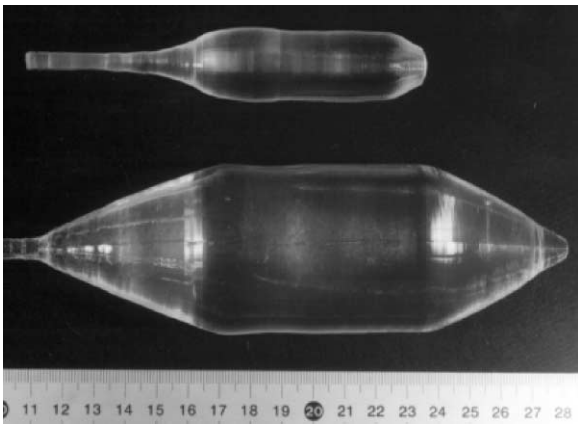

Fig. 6. As-grown 2″ diameter Ce-doped $LiCaAlF_6$ single crystal.

Fig. 6 shows an as-grown 2″ diameter Ce : LiCAF single crystal, free from cracks and inclusions. By improving the growth conditions, such as the precise control of crystal diameter to avoid the formation of inclusions and the termination of crystal growth at the solidification fraction of 60%

to avoid the formation of the white substance at the bottom of crystal, crystals shown in Fig. 6 could be obtained reproducibly. 2″ diameter undoped LiCAF single crystals could also be grown under the same conditions as Ce : LiCAF single crystals. Fig. 7 shows a wafer cut perpendicular to the growth axis of the undoped LiCAF single crystal.

Fig. 8 shows the distribution of bi-refringence among wafers of LiCAF single crystals. Since the deviation of bi-refringence among wafer was in the order of 10 nm/mm, it has sufficient quality as a preliminary experiment. Fig. 9 shows the transmission spectra of the LiCAF and LiSAF single crystals. Dotted lines correspond to the spectra of LiCAF and LiSAF grown under Ar atmosphere. The crystal growth chamber was evacuated to 10^{-2} Torr prior to the crystal growth. A solid line corresponds to the spectrum of the LiCAF single crystals grown in this work, under CF_4 atmosphere. The crystal growth chamber was evacuated to 10^{-5} Torr prior to the crystal growth. It was clearly shown that the crystal growth conditions largely affect the transmission property. The absorption at around 125 nm, which was observed in crystals grown under Ar atmosphere and might be due to a color center or impurity, could be eliminated by changing the growth atmosphere to CF_4 and the degree of vacuum prior to the growth. The absolute transmittance itself could be well modified. Further investigations should be done taking into account the surface conditions of wafers and reflection from the wafer surface. These transmission characteristics of LiCAF show their high potential as optical window materials in the UV and VUV wavelength region.

Recently, there has been significant interest in using 157-nm laser sources in projection lithography as successors to 193-nm-based systems. This

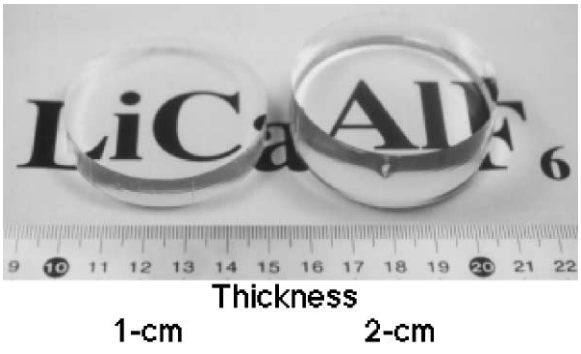

Fig. 7. Wafers cut perpendicular to the growth axis of the undoped $LiCaAlF_6$ single crystal.

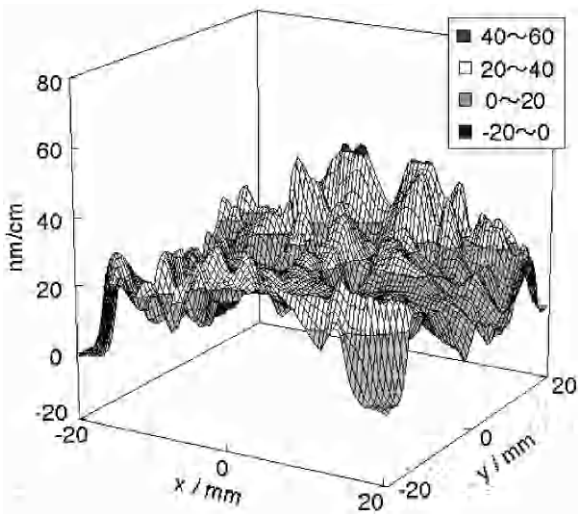

Fig. 8. Bi-refringence distribution among the undoped $LiCaAlF_6$ wafers.

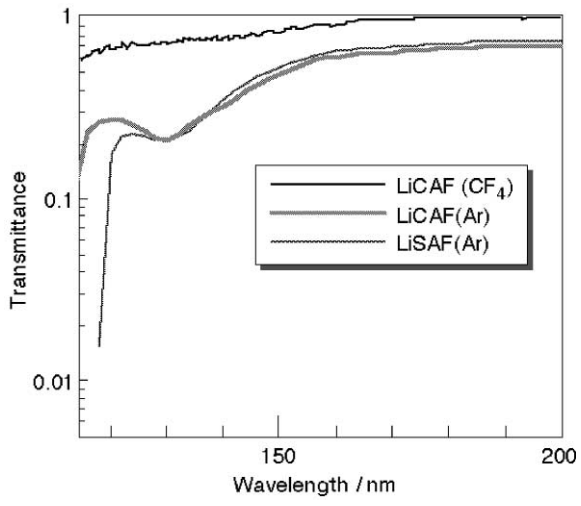

Fig. 9. Transmission spectra of un-doped $LiCaAlF_6$ and $LiSrAlF_6$ single crystals in the vacuum-ultra-violet wavelength region.

would follow the historical trends in the industry, where wavelength reduction has been used to improve feature resolution and process latitude. One of the most serious problems in realizing a 157-nm-based system is the development of suitable optical materials for lenses and other optical components. Although 248- and 193-nm-based systems could be realized using fused silica and CaF_2, a new material is required for 157-nm-based systems because of the limitation of fused silica transparency. In fact, a 2-mm-thick UV-grade fused silica plate transmits less than 10% at 157 nm [11]. In particular, for an all-refractive design 157-nm laser source, a second material other than CaF_2 is strongly required, because CaF_2 is the most promising material to be used. Primary candidates for a second material were LiF and MgF_2; however, they have several disadvantages such as a fragile and hygroscopic nature and large bi-refringence [12].

The problems of optical materials used for UV and VUV are the limited transmission and the difficulty of material processing and polishing due to cleavage, or the hydroscopic nature of the material. LiCAF does not have these problems, and therefore will be a suitable optical material for the UV and VUV regions, becoming much more important in the next generation of lithographic technology.

4. Summary

Ce : LiCAF and Ce : LiSAF crystals 25 mm in diameter were grown by the CZ technique under CF_4 atmosphere. Ce : LiSAF showed a tendency to crack more easily than Ce : LiCAF. Although lattice parameters of both the *a*- and *c*-axis increased linearly depending on a temperature in the case of LiCAF, that of the *c*-axis decreased in the case of LiSAF. Linear thermal expansion coefficients of both LiCAF and LiSAF were evaluated using the temperature dependence of the lattice parameter. Under the same growth conditions, Ce-doped and undoped LiCAF 50 mm diameter (2″) single crystals were also grown up to a solidification fraction of 60%. Although numerous inclusions appeared during growth, precise diameter control prevented their formation. Undoped LiCAF single crystals grown under CF_4 atmosphere showed better transmission properties in the UV and VUV wavelength regions, such as higher transmittance and no degrading absorption peak at around 125 nm, than crystals grown under Ar atmosphere. These characteristics indicate the high potential of these crystals as optical window materials.

References

[1] M.A. Dubinskii, V.V. Semashko, A.K. Naumov, R.Y. Abdulsabirov, S.L. Korableva, Laser Phys. 3 (1993) 216.
[2] C.D. Marshall, S.A. Payne, J.A. Speth, W.F. Krupke, G.J. Quarles, V. Castillo, B.H.T. Chai, J. Opt. Soc. Am. B. 11 (1994) 2054.
[3] K. Shimamura, S.L. Baldochi, N. Mujilatu, K. Nakano, Z. Liu, H. Ohtake, N. Sarukura, T. Fukuda, J. Crystal Growth 211 (2000) 302.
[4] K. Shimamura, N. Mujilatu, K. Nakano, S.L. Baldochi, Z. Liu, H. Ohtake, N. Sarukura, T. Fukuda, J. Crystal Growth 197 (1999) 896.
[5] Z. Liu, K. Shimamura, K. Nakano, T. Fukuda, T. Kozeki, H. Ohtake, N. Sarukura, Jpn. J. Appl. Phys. 39 (2000) L466.
[6] S.L. Baldochi, K. Shimamura, K. Nakano, N. Mujilatu, T. Fukuda, J. Crystal Growth 200 (1999) 521.
[7] S.L. Baldochi, K. Shimamura, K. Nakano, N. Mujilatu, T. Fukuda, J. Crystal Growth 205 (1999) 537.
[8] I.M. Ranieri, K. Shimamura, K. Nakano, T. Fujita, L.C. Courrol, S.P. Morato, T. Fukuda, J. Crystal Growth 217 (2000) 145.
[9] I.M. Ranieri, K. Shimamura, K. Nakano, T. Fujita, Z. Liu, N. Sarukura, T. Fukuda, J. Crystal Growth 217 (2000) 151.
[10] D. Klimm, P. Reiche, Proceedings of International Symposium on Laser and Nonlinear Optical Materials, 3–5 November 1997, p. 284.
[11] T.M. Bloomstein, V. Liberman, M. Rothschild, D.E. Hardy, R.B. Goodman, Proceedings of the Emerging Lithographic Technologies III, SPIE, Vol. 3676, 1999, p. 342.
[12] T.M. Bloomstein, M.W. Hom, M. Rothschild, R.R. Kunz, S.T. Palmacol, R.B. Goodman, J. Vac. Sci. Technol. B 15 (1997) 2112.